Journal of Biomedical Optics

SPIEDigitalLibrary.org/jbo

Multichannel scan surface plasmon resonance biochip with stationary optics and baseline updating capability

Cheng Wang
Ruping Liu
Wei Zhang
Yujian Wang
Kai Xu
Zhao Yue
Guohua Liu

SPIE

Multichannel scan surface plasmon resonance biochip with stationary optics and baseline updating capability

Cheng Wang,[a,b] Ruping Liu,[a,c] Wei Zhang,[a,d] Yujian Wang,[a] Kai Xu,[a] Zhao Yue,[a] and Guohua Liu[a]
[a]Nankai University, Department of Electronics and Microelectronics, Tianjin 300071, China
[b]Columbia University, Department of Mechanical Engineering, New York 10027
[c]Beijing Institute of Graphic Communication, School of Printing and Packaging Engineering, Beijing 102600, China
[d]Nankai University, Electronic Information Laboratorial Teaching Center, Tianjin 300071, China

Abstract. An on-chip spectral surface plasmon resonance (SPR) biosensor with three parallel channels has been built for biomolecule detections. It is capable of updating intensity baselines to suppress errors induced by light source instability. In order to minimize structure and reduce positional regression uncertainty, the scan operations are achieved by timely changing optical media instead of conventional mechanical scan. The detection results of human immunoglobulin G (hIgG) demonstrated that the baseline updating improves the limitation of detection of hIgG concentration from ~86.1 to ~17.4 ng/mL. [DOI: 10.1117/1.JBO.18.11.115002]

Keywords: surface plasmon resonance; biochip; multichannel; baseline updating; nonmovement scan.

Paper 130644R received Sep. 4, 2013; revised manuscript received Oct. 2, 2013; accepted for publication Oct. 9, 2013; published online Nov. 5, 2013.

1 Introduction

Nowadays, analytical devices have shown minimization and integration trends. Different from routine analytical methods represented by tube and microtiter plate, the micrometer-scale total analysis systems (μTAS) or so called lab-chip devices, which integrate novel sensing units and offer significant advantages, such as miniaturization, saving of analyte samples, low power consumption, on-site testing, and rapidity of assay, have attracted more and more interest.[1] In this work, the authors present a spectral surface plasmon resonance (SPR) sensor based biochip device.

Spectral SPR sensors have become widely utilized analytical tools in biomedical research due to high performance and easy applications by using commercial spectrometer instruments.[2] For multianalyte detection and parallel reference assay capabilities, sensor systems are usually designed as multichannel structures. Multichannel scan mechanisms, which employ wavelength-division multiplexing,[3] multiple fiber receptors,[4] and mechanical movement of optics,[5] have been reported. However, these methods lead to complicated structures, more components, larger device sizes, and even induce positional regression uncertainty errors, and thus impair the convenience in on-site biomedical measurements.[6] In order to alleviate these drawbacks, we designed a simple and compact multichannel SPR biochip. By using a completely nonmovement scan mechanism, three parallel channels can be scanned in time-division approach. Specially, we proposed that by exclusively using one channel to detect air, the device can provide the baseline updating capability to suppress detection errors arising from the light source instability. The device performances in biomedical sensing were demonstrated by a representative detection of human immunoglobulin G (hIgG). The results illustrated that with the baseline updating, the device provides an ideal resolution on target analyte concentration.

Address all correspondence to: Guohua Liu, Nankai University, Department of Electronics and Microelectronics, Tianjin 300071, China. Tel: +86 22 23501565; Fax: +86 22 23501565; E-mail: liugh@nankai.edu.cn

2 Materials and Methods

2.1 *Device*

The device under the Kretschmann configuration is shown in Fig. 1. The metal film (5 nm Cr and 45 nm Au) is deposited on the BK7 glass ($n_{BK7} = 1.5168$) substrate, and three parallel channels are divided on it. Above the substrate is a FK5 glass ($n_{FK5} = 1.4875$) input optical path. In order to achieve multichannel scan without optics movements, a rectangular matching liquid chamber (10-mm length, 0.5-mm width, and 1-mm height) was designed on the FK5 optical path, as shown in Figs. 1(a) and 1(b). By changing the refractive index (RI) value of matching liquid in chamber, the incident beam can be led into different SPR channels. In our device, an AC voltage controlled piezoelectric micropump [Fig. 1(c)] was used to drive matching liquids accurately.[7,8] Control voltages with different frequencies can drive different matching liquids into the chamber.

Based on previous work,[8] we know that if the beam inputs with a special angle $\alpha_i = 72.17$ deg, after two refractions (enters the matching liquid from FK5 glass and leaves the matching liquid to BK7 glass), the incident SPR angle can be adjusted to an appropriate value $\alpha_o = 69$ deg:[9]

$$\alpha_o = \arcsin\left(\sin\ \alpha_i \cdot \frac{n_{FK5}}{n_{BK7}}\right) = \arcsin\left(\sin\ 72.17\ \text{deg} \cdot \frac{1.4875}{1.5168}\right) \cong 69\ \text{deg}.$$

Matching liquids with different RI values provide same α_o [assume RI value is large enough to avoid the total reflection (TR)], but different horizontal shifts l_k:

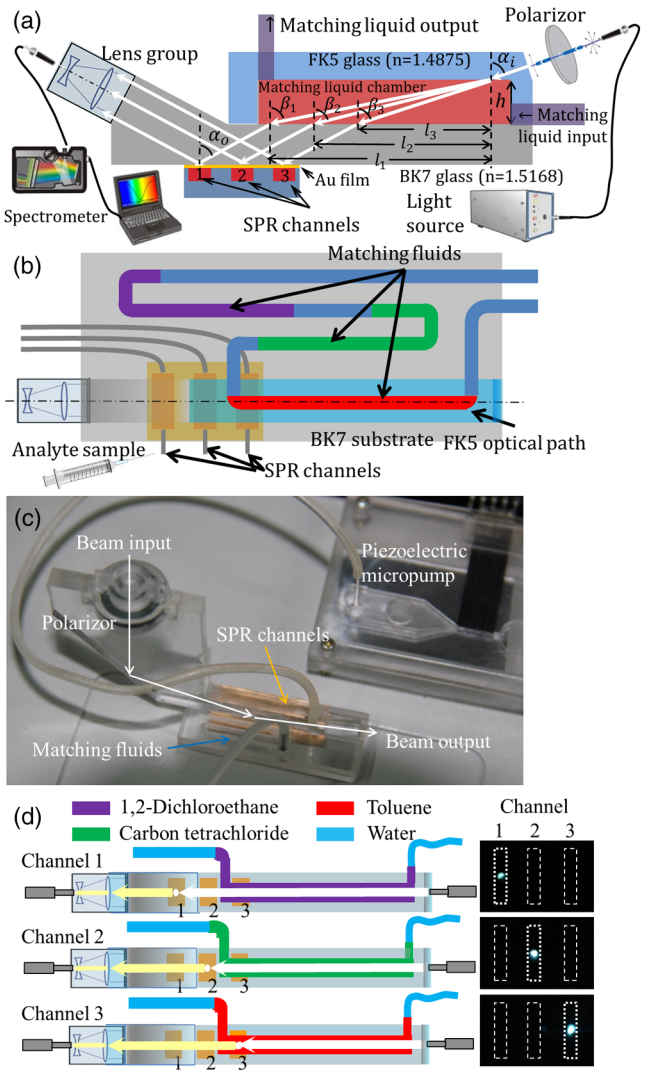

Fig. 1 Structure of device. (a) Side view of device and optical paths. (b) Vertical view of device and distribution of matching liquids. (c) Photograph of the device. (d) Scan states (purple: matching liquid is $C_2H_4Cl_2$, scanning channel 1; green: matching liquid is CCl_4, scanning channel 2; red: matching liquid is C_7H_8, scanning channel 3).

$$l_k = \tan\left[\arcsin\left(\sin\alpha_i \cdot \frac{n_{\mathrm{FK5}}}{n_k}\right)\right] h = \tan\left[\arcsin\left(\frac{1.4161}{n_k}\right)\right] h,$$

where n_k is the RI value of matching liquids and h is the height of matching liquid chamber. By timely changing matching liquids, the beam can be correspondingly deflected with different l_k. In this work, three colorless and transparent organic solvents are used as matching liquids: 1, 2-dichloroethane ($n_1 = 1.4448$), carbon tetrachloride ($n_2 = 1.4601$), and toluene ($n_3 = 1.4969$), water segments exist between organic matching liquids to prevent volatilizing and mutual mixing. Corresponding l_k values are $l_1 = 4.9420$ mm, $l_2 = 3.9807$ mm, and $l_3 = 2.9189$ mm, respectively. The spans around 1 mm between each other are sufficient to arrange three parallel SPR channels. The photographs taken from the back side of the substrate [Fig. 1(d)] confirmed that the beam can be led to correct SPR channels.

2.2 *Sensitive Film*

For hIgG detections, we built a hIgG-sensitive film on the Au surface.[10] The Au film was in turn immersed in a 20-mM 11-mercaptoundecanoic acid (MUA, J&K Chemical, Beijing, China) methanolic solution (5 h), an equal volume mixture of 20-mM 1-ethyl-3-[3-dimethylaminopropyl] carbodiimide hydrochloride (EDC, Alfa Aesar, Ward Hill, Massachusetts) and 50-mM *N*-hydroxysuccinimide (NHS, Alfa Aesar, Ward Hill, Massachusetts) aqueous solutions (5 h), a 100-μg/mL streptavidin (Sigma Aldrich, St. Louis, Missouri) phosphate buffered saline (PBS) solution (1 h), and a 300 μg/mL goat anti-hIgG (Sigma Aldrich, St. Louis, Missouri) PBS solution (2 h). Then, a 2-mg/mL bovine serum albumin (BSA, Sigma Aldrich, St. Louis, Missouri) PBS solution was used to block the excess reactive groups (30 min). All operations above were operated at room temperature.

3 Experiments

In this work, we used light source DH-2000-BAL, optical fiber P50-2-UV-VIS, and spectrometer Maya-2000 Pro (Ocean Optics products, Dunedin, Florida) to detect reflective intensity distribution on the spectrum from 550 to 1050 nm. The spectrometer grating is HC-1, the slit width is 250 μm, and the integration time is 20 ms.

Our device detects hIgG affinity by localizing the resonance wavelength of spectrogram SPR-dip, which equals the ratio between the attenuated total reflection (ATR) spectrum of hIgG solution and the incident beam spectrum (baseline).[2] Because of the incident spectrum measurement needs an additional photodetector; we chose the ATR spectrum of air (air baseline) approximately instead of the baseline. Our reason is that the resonance wavelength of air is ~500 nm, in the resonance wavelength band of aqueous solutions (~740 nm) is very close to the TR spectrum. Then, the SPR-dip with a typical shape can be fitted by the Lorentzian equation to calculate the accurate resonance wavelength:[11]

$$R(\lambda) = 1 - A\frac{W + P(\lambda - C)}{W^2 + (\lambda - C)^2},$$

where A relates to the depth, P to the asymmetry, C to the position, and W to the width of the SPR-dip.

When a single channel is used to detect liquid samples, the air baseline only can be obtained before experiments; once liquid is in channel, it cannot be acquired any more. Consider that the air baseline inevitably drifts along with time, thus the liquid sample's ATR spectrum also unpredictably drifts; the prestored air baseline without timely refreshment may lead to the SPR-dip distortions. In order to get rid of drift influences, we used an independent channel to supply a timely refreshed air baseline.[12]

In hIgG detections, we functionalized channel 1 with sensitive film to detect surface-specific affinity of hIgG, channel 2 (naked Au film) was full of air to provide baselines, and channel 3 (naked Au film) was used to detect nonspecific affinity responses. The hIgG PBS solutions at low concentrations of 5, 10, 50, 100 ng/mL were detected, respectively. The scan sequence among three channels is: $1 \rightarrow 2 \rightarrow 3 \rightarrow 2 \rightarrow 1$ and circulate so on. Every spectrum collected from channel 2 provides the air baseline for the last channel scanned before channel 2. The time interval between every two neighboring scans is 15 s. In every minute, both channels 1 and 3 are scanned

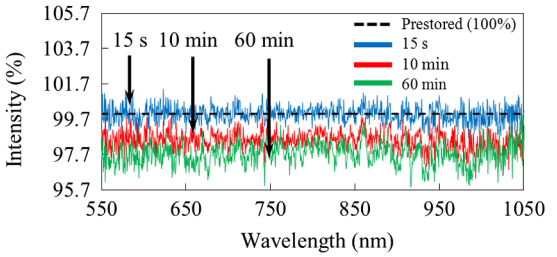

Fig. 2 Air baseline drifts.

once, and channel 2 provides two updated baselines for each of them.

Table 1 Statistics of wavelength responses.

	Response (no baseline updating)		Response (baseline updating)	
c_{hIgG} (ng/mL)	$\overline{\Delta\lambda}$ (nm)	σ (nm)	$\overline{\Delta\lambda}$ (nm)	σ (nm)
5	58.758	0.140	58.096	0.019
10	58.832	0.125	58.153	0.027
50	59.069	0.143	58.298	0.022
100	59.244	0.143	58.555	0.023

4 Results and Discussion

First, we observed the air baseline drifts from channel 2. In Fig. 2, three curves are acquired by comparing three air baselines ($t = 15$ s, 10 min, 60 min) with the prestored air baseline. The amplitude averages of spectra are 0.9998, 0.9851, and 0.9769. Noise standard deviations are 0.0046, 0.0050, and 0.0062. If the air baseline does not drift, spectra should keep flat and constant amplitudes at 100% (black dotted line in Fig. 2). However, they show inconsistent fluctuations at different wavelengths. Hence, we learned that the drift leads to continuously increasing errors and impairs the localizing accuracy of resonance wavelength. In addition, we also found that the drift is not rapid; the air spectrum at $t = 15$ s shows high similarity to the prestored air baseline. Therefore, we confirmed that the air baseline updating with 15-s delay still can improve the drift influences.

The hIgG responses with and without baseline updating are shown in Fig. 3, respectively. When the baselines were not timely

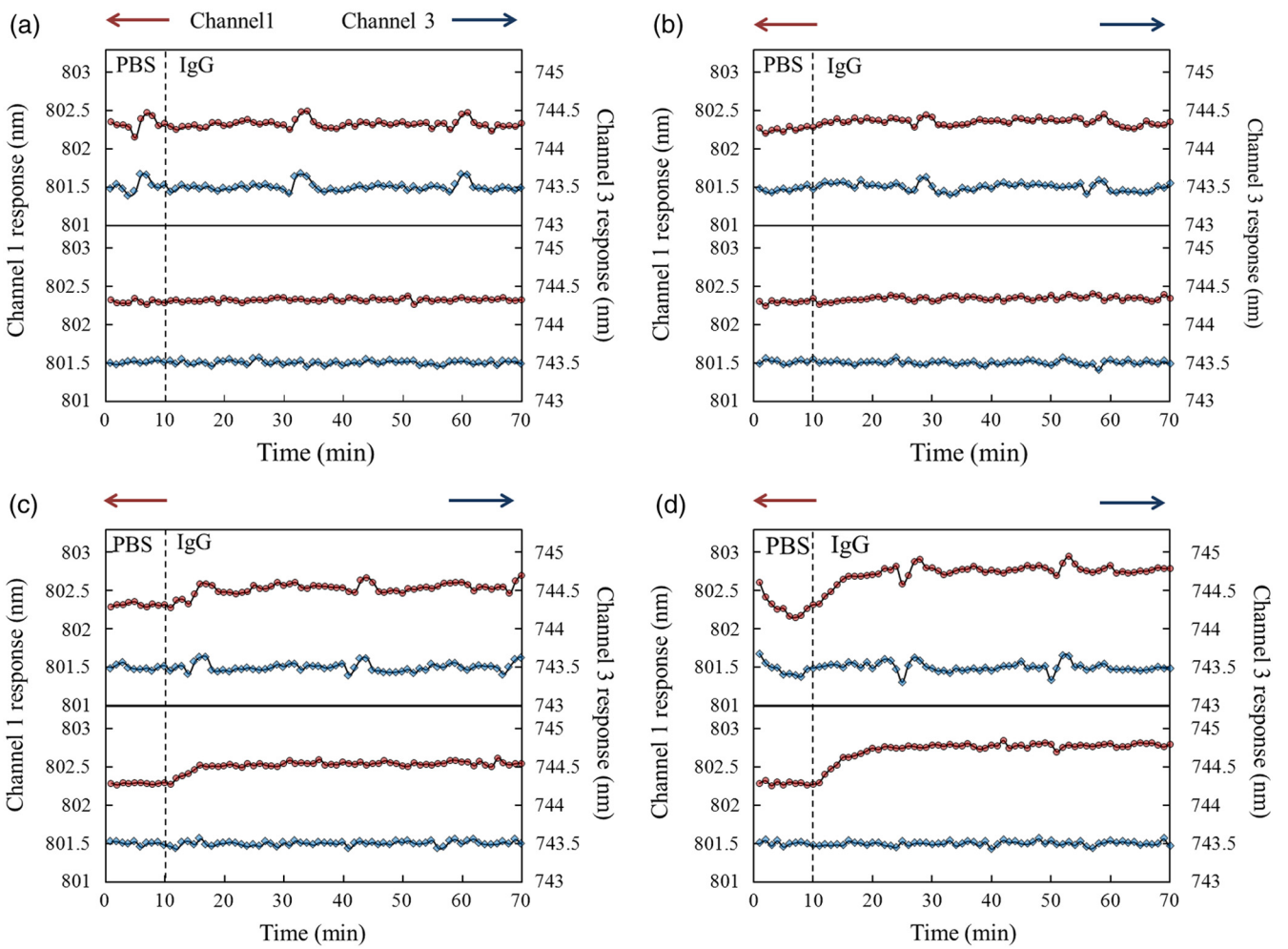

Fig. 3 SPR responses at different human immunoglobulin G (hIgG) concentrations. (a) 5 ng/mL. (b) 10 ng/mL. (c) 50 ng/mL. (d) 100 ng/mL. In every plot, the upper subpanel is response without baseline updating, the lower subpanels is response with baseline updating. In every subpanel, the red-dot curve is the specific response from channel 1, the blue-diamond curve is the nonspecific response from channel 3.

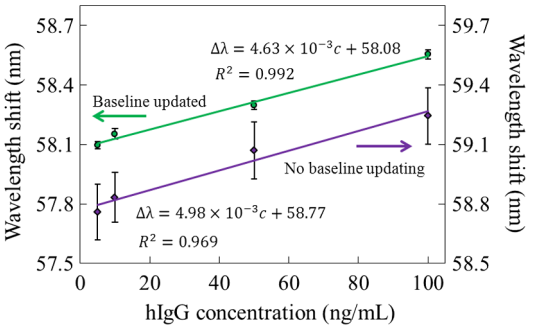

Fig. 4 Relationships between hIgG concentration and SPR equilibrium response (purple: no baseline updating; green: with baseline updating).

updated, the SPR responses [upper subpanels in Fig. 3(a)–3(d)] show severe noises both in the specific channels (red curves) and the nonspecific channels (blue curves). If hIgG concentration is very low [Figs. 3(a) and 3(b)], the specific responses can hardly be identified. Particularly, the noisy responses from channel 1 and channel 3 show periodical vibrations and highly correlative waveforms. Based on these phenomena, we considered that the noises may stem from the light source instability and they could be suppressed by timely updating baseline. The SPR responses with updated baselines are shown in the lower subpanels in Figs. 3(a)–3(d)]. It is easy to learn that response performances have been significantly improved.

The detailed statistical information of Fig. 3 is given in Table 1. For presenting the SPR responses of hIgG-specific interactions on the sensitive film surface (eliminating nonspecific absorption and bulk response effects), we chose $\Delta\lambda$, the relative shift of resonance wavelength responses from channel 1 (specific responses) and channel 3 (nonspecific responses), as the output. Without timely baseline updating, the largest standard deviation wavelength responses are 0.143 nm. By using updated baselines, the largest standard deviation is decreased to 0.027 nm.

Further, we know that the relationship between $\Delta\lambda$ and hIgG concentration c can be described by Langmuir absorption isotherm.[13] When c is very low, it can be deemed to an approximately proportional relationship:

$$\Delta\lambda = k \cdot \lim_{t\to\infty} r(t) + d = k \cdot \frac{c}{c + K_D} + d \cong k \cdot \frac{c}{K_D} + d = S \cdot c + d,$$

where $\lim_{t\to\infty} r(t)$ is the equilibrium binding rate, K_D is the equilibrium dissociation constant, S is the sensitivity, and d is the intercept.

Two linear fitting lines are presented in Fig. 4. Without baseline updating (bule line), the fitting goodness is $R^2 = 0.969$. The sensitivity (slope) is $S \simeq 4.976 \times 10^{-3}$ nm/(ng/mL). Thus, the concentration resolution[2] of hIgG can be estimated by the worst standard deviation: $\sigma_c = \sigma/S = 0.143/(4.976 \times 10^{-3}) \cong 28.7$ ng/mL. Referring to the "3σ" rule, the limitation of detection (LOD) of hIgG can be defined as: LOD $= 3\sigma_c =$ 86.1 ng/mL. Correspondingly, with the baseline updating, $R^2 = 0.999$ and $S \cong 4.628 \times 10^{-3}$ nm/(ng/mL). The new concentration resolution is enhanced up to $\sigma_c = \sigma/S = 0.027/(4.628 \times 10^{-3}) \cong 5.8$ng/mL and LOD$=3\sigma_c \cong 17.4$ng/mL.

5 Conclusion

In summary, we developed an on-chip multichannel spectral SPR device for biomedical detections. Experimentally, we demonstrated that the novel nonmovement scan design simultaneously provides specific reaction responses, nonspecific responses, and updated baselines. With timely updated baselines, noises due to the light intensity fluctuation can be efficiently suppressed. Hence, the device gives a highly improved LOD of hIgG. Compare to conventional multichannel scan mechanisms, here the parallel scan, which is achieved by optical media changing, overcomes the positional regression uncertainty and makes the device simpler and more reliable.

Acknowledgments

This work is supported by Natural Science Foundation of China (61271099), Natural Science Foundation of Tianjin (12JCZDJC20400), and National Research Foundation for Doctoral Program of Higher Education of China (20120031110031). Besides, C.W. appreciates the national scholarship (201206200032) from China Scholarship Council.

References

1. D. Janasek, J. Franzke, and A. Manz, "Scaling and the design of miniaturized chemical-analysis systems," *Nature* **442**(7101), 374–380 (2006).
2. M. Piliarik and J. Homola, "Surface plasmon resonance (SPR) sensors: approaching their limits?," *Opt. Express* **17**(19), 16505–16517 (2009).
3. J. Dostálek, H. Vaisocherová, and J. Homola, "Multichannel surface plasmon resonance biosensor with wavelength division multiplexing," *Sensor Actuator B: Chem.* **108**(1), 758–764 (2005).
4. J. Homola et al., "A novel multichannel surface plasmon resonance biosensor," *Sensor Actuator B: Chem.* **76**(1), 403–410 (2001).
5. J. Homola et al., "Multi-analyte surface plasmon resonance biosensing," *Methods* **37**(1), 26–36 (2005).
6. B. Sutapun et al., "A multichannel surface plasmon resonance sensor using a new spectral readout system without moving optics," *Sensor Actuator B: Chem.* **156**(1), 312–318 (2011).
7. W. Zhang et al., "Travelling-wave piezoelectric micropump with low resistance microchannel," *Electron. Lett.* **47**(19), 1065–1066 (2011).
8. C. Wang et al., "Time-division self-referencing multichannel spectral SPR sensor without mechanical scanning," *Electron. Lett.* **49**(7), 493–495 (2013).
9. G. Gupta and J. Kondoh, "Tuning and sensitivity enhancement of surface plasmon resonance sensor," *Sensor Actuator B: Chem.* **122**(2), 381–388 (2007).
10. E. C. A. Stigter, G. J. de Jong, and W. P. Van Bennekom, "An improved coating for the isolation and quantitation of interferon-γ in spiked plasma using surface plasmon resonance (SPR)," *Biosens. Bioelectron.* **21**(3), 474–482 (2005).
11. P. Tobiška and J. Homola, "Advanced data processing for SPR biosensors," *Sensor Actuator B: Chem.* **107**(1), 162–169 (2005).
12. F. Bardin et al., "Surface plasmon resonance spectro-imaging sensor or biomolecular surface interaction characterization," *Biosens. Bioelectron.* **24**(7), 2100–2105 (2009).
13. D. R. Gondim et al., "Dye ligand epoxide chitosan/alginate: a potential new stationary phase for human IgG purification," *Adsorpt. Sci. Technol.* **30**(8), 701–712 (2012).